Modeling Earth Systems and Environment
https://doi.org/10.1007/s40808-023-01848-6

ORIGINAL ARTICLE

# Solar radiation variability across Nigeria's climatic zones: a validation and projection study with CORDEX, CMIP5, and CMIP6 models

Christiana Olusegun[1,2] · Olusola Ojo[3] · Adeyemi Olusola[4] · Samuel Ogunjo[3]

Received: 2 January 2023 / Accepted: 14 August 2023


## Abstract
Harnessing energy from the sun is crucial for locations battling with energy poverty and generation, especially in Africa, where equity in energy distribution and generation is a daily challenge. However, the evaluation and analysis of solar radiation has been limited by the paucity of atmospheric data in the African region. This study used monthly downward surface solar radiation (SSRD) from ERA5 as reference data to evaluate simulations of solar radiation from CORDEX, CMIP5 and CMIP6 models spanning the period 1990−2020 (present-day), mid-future (2020−2050), and far-future (2070−2100) across 4 climatic zones (Coastal, Forest, Guinea and Sahel) in Nigeria. Solar radiation were found to be overestimated in the Guinea and Sahel zones of the country, but fairly good performance were made in the Coastal and Forest zones. CMIP5, CMIP6 and CORDEX individual models all exhibit strong agreement in the projection of solar dimming across the four climatic zones in the mid- and far-future under both RCP4.5/SSP5−4.5 and RCP8.5/SSP5−8.5 scenarios. However, under the RCP8.5/SSP5−8.5 the greatest magnitude of dimming ($-35W/m^2$) was found in CMIP6 models in the far-future and ($-12W/m^2$) in the mid-future. The projected solar dimming was also predominant in all climatic regions under SSP5−4.5 for CORDEX, CMIP5, and CMIP6 models but at a much lower magnitude.

**Keywords** Climate change · Solar radiation · CMIP6 · Nigeria · CORDEX

## Introduction

The significance of solar radiation cannot be overstated in relation to its intensity, distribution, and future variability. This is especially true for areas struggling with energy poverty and generation. Solar radiation is important for human livelihoods and the survival of ecosystems on Earth (Diaci 1999). In order to effectively manage issues surrounding socioeconomic growth, industrialization, and economic production, adequate knowledge of solar radiation is crucial, especially for developing economies worldwide. For instance, solar energy offers a clean and sustainable energy alternative that diminishes dependency on fossil fuels and also aids in curbing greenhouse gas emissions, thereby facilitating a transition toward a greener and more sustainable energy landscape. However, equitable energy distribution and generation in West African countries have been a daily challenge, resulting in variations in per capita energy supply and demand (Avila et al. 2017; Iwayemi and Iwayemi 1998). For developing nations such as Nigeria grappling with energy supply challenges, the key to surmounting these obstacles lies in their ability to accurately quantify solar

✉ Christiana Olusegun
chrystali2002@gmail.com

Olusola Ojo
ojoso@futa.edu.ng

Adeyemi Olusola
aolusola@yorku.ca

Samuel Ogunjo
stogunjo@futa.edu.ng

[1] Doctoral Research Program-West African Climate System (DRP-WACS), West African Science Service Centre on Climate Change and Adapted Land Use (WASCAL), Federal University of Technology Akure, Ilesha-Owo Expressway, Akure 340001, Ondo State, Nigeria

[2] Faculty of Physics, University of Warsaw, Ludwika Pasteura 5, 02-093 Warsaw, Mazowieckie, Poland

[3] Department of Physics, Federal University of Technology Akure, Ilesha-Owo Expressway, Akure 340001, Ondo State, Nigeria

[4] Faculty of Environmental and Urban Change, York University, 4700 Keele St, Toronto, ON M3J 1P3, Canada

Published online: 31 August 2023

intensity, a fundamental factor in harnessing solar energy effectively. By acquiring comprehensive data on solar radiation, these countries can lay the groundwork for informed decision-making, strategic planning, and the successful implementation of solar power systems, consequently bolstering their energy security, promoting economic growth, and improving the quality of life for their population. Hence, knowledge of solar intensity per unit area is a major step for any country looking to tap into the vast amount of renewable energy available in the form of solar radiation (El Mghouchi et al. 2016; Nešović 2022, 6). In Nigeria, the lack of in-situ measurements and data structures for solar radiation makes reliability on reanalysis and numerical model simulations an alternative for solar radiation studies. By leveraging these alternatives, Nigeria can still access valuable insights into solarsabah7modeling radiation patterns and distributions, facilitating informed decision-making processes, energy planning, and advancing solar energy infrastructure in the country.

The future of solar energy utilization in West African countries, particularly Nigeria, is heavily based on accurate projections of solar radiation. However, with the increasing availability of open-source Earth Observation products, cloud computing platforms, and advanced computational capabilities, promising avenues exist for modelling and projecting future climatological parameters such as solar radiation. This presents a unique opportunity to generate renewable energy and analyze crucial energy budgets. These advancements hold immense potential for advancing the understanding of solar radiation and its implications in the region, particularly in addressing energy poverty in Nigeria and other West African countries Edomah et al. (2021); Chanchangi et al. (2022). Although there are challenges in accurately projecting solar radiation due to factors such as cloud cover, aerosol loading, and wind speed, our study aims to improve our understanding of long-term solar radiation patterns in Nigeria and examine its prospects using reanalysis data to validate the solar radiation output obtained from numerical modelling techniques. This research fills a gap in previous studies (Ogunjo et al. 2022; Salaudeen et al. 2021) that have predominantly focused on validating precipitation, temperature, and other weather variables but have given limited attention to validating solar radiation specifically.

A major advantage is the ability of reanalysis and numerical climate models to estimate solar radiation in areas without long-term measurement and provide future projections at a country-level scale. This is particularly important since in-situ solar radiation measurements are often not freely available globally or at a country level. However, there are inherent uncertainties associated with using the reanalysis/numerical models approach. As a result, it is important to validate these models with ground observation, which can be achieved by establishing experimental test sites in different country zones. ERA-5, the most recent atmospheric reanalysis product from The European Centre for Medium-Range Weather Forecasts (ECMWF), is a reliable source of hourly estimates of many atmospheric, land, and oceanic climate variables Hersbach et al. (2020). Studies conducted in different parts of the world have found ERA5 to be relatively good in comparison to ground observation, with low relative mean bias error (e.g Babar et al. (2019); Trolliet et al. (2018); Urraca et al. (2018); Tahir et al. (2020). For instance, the performance of ERA5 for solar radiation data is better than six other reanalysis datasets over Pakistan Tahir et al. (2020). The reliability of ERA5 datasets has also been established in other regions of the world. Climate scientists employ global circulation models (GCMs) and regional climate models (RCMs) to access historical conditions and project future climatic conditions/patterns globally at various resolutions.

The World Climate Research Program's Coupled Model Intercomparison Project (CMIP) offers extensive global-scale climate simulations. CMIP6 and CMIP5 represent two project phases comprising numerous climate models worldwide, simulating various atmospheric variables at different spatiotemporal resolutions (Eyring et al. 2016; Taylor et al. 2012). CMIP6, the latest phase, incorporates advancements in model development, enhanced representation of Earth system processes, and updated future climate scenarios compared to CMIP5. With more accurate and detailed simulations of climate variables and their interactions, CMIP6 models enable improved projections of climate change impacts. The outcome of this study will also depict the extent of improvements in CMIP6 compared to CMIP5, specifically for solar radiation estimations in Nigeria, building upon the progress made in the previous phase while addressing identified limitations and challenges. Similarly, the Coordinated Regional Climate Downscaling Experiment (CORDEX), also led by the WCRP, focuses specifically on regional climate modelling and GCMs downscaling, enabling more detailed assessments at finer spatial scales compared to GCMs like CMIP6 and CMIP5. These numerical modelling approaches allow researchers to extend their analyses beyond historical data and generate projections that offer insights into future climate dynamics and potential impacts. These collaborative efforts among climate scientists worldwide continue to advance our understanding of climate dynamics and projections.

In Nigeria, the lack of long-term solar radiation measurements has made it difficult to evaluate and plan for sectors such as energy and agriculture. Although developing countries like Nigeria are interested in utilizing solar energy, Africa's scarcity of atmospheric data presents challenges. This study aims to assess different numerical models and determine changes in solar radiation under various climate scenarios using CORDEX, CMIP5, and CMIP6 models. The results will provide reliable historical data and insights into future solar radiation patterns, enabling regional stakeholders to develop climate change adaptation and mitigation policies. However, accurate simulation of the present or historical patterns is necessary to project future climate projections for solar radiation due to continuous development and improvements in climate models.

## Methodology

Solar radiation is significant in Earth's energy budget and is pivotal in numerous climatic and environmental processes. Accurate solar radiation measurement is crucial for various applications, including assessing renewable energy resources, climate modelling, and agricultural planning. In this methodology, we present a comprehensive approach to validate solar radiation data by leveraging ERA5 reanalysis data as the reference dataset and comparing it with CMIP6, CMIP5, and CORDEX model data.

### ERA5 as reference observation

Monthly surface solar radiation downward (SSRD) from ERA5 Hersbach et al. (2020), at a high spatial resolution of $0.1^o \times 0.1^o$ for the period spanning $1990 - 2020$ was used as the reference data over the region of study. SSRD gives information on the amount of shortwave radiation (direct and diffuse) reaching the surface of the Earth. It is an essential variable for understanding the energy balance of the Earth's surface. It is crucial in various applications such as renewable energy assessment, climate modelling, and agricultural planning. It is derived from satellite observations, ground-based measurements, and advanced numerical models. The data is obtained via the Copernicus Climate Data Store (https://cds.climate.copernicus.eu/cdsapp#!/dataset/reanalysis-era5-single-levels-monthly-means?tab=form, allowing scientists to analyze and study solar radiation patterns and variability across different regions and periods. The unit of SSRD is then converted to $W/m^2$ from $J/m^2$ for comparison with the model data.

### Model selection and description

Model simulations of surface downwelling shortwave radiation (RSDS) were obtained from CORDEX-AFR-44, CMIP5, and CMIP6 experiments to provide additional information for present-day climate and future projections over the study area. RSDS is the sum of direct and diffuse solar radiation incident on the surface and is sometimes called "global radiation" http://vocab.nerc.ac.uk/collection/P07/current/CFSN0275/. The selection of models from CORDEX, CMIP5, and CMIP6 experiments is based on the availability of RSDS simulation for present-day climate and its associated RCP4.5/SSP245 and RCP8.5/SSP585 scenarios. In this paper, we focus on analyzing the present-day climate from $1990 - 2020$, even though the CMIP6 historical runs encompass the time period of 1850 to 2014. This choice ensures that the analysis reflects consistent contemporary climate conditions, trends, and potential changes immediately relevant to current research objectives. Further constraints considered include using only the first ensemble member r1i1p1f1 model variant and data availability to fulfil the selection criteria. Accordingly, this study selected a total of 15 models from Africa-CORDEX (hereafter refer to as CORDEX), and 16 models from both CMIP5 and CMIP6 experiments all met the specified criteria outlined earlier (refer to Tables 1, 2, 3). These models were subjected to further analysis.

The choice of the inherent radiative scheme within numerical climate models holds significant relevance when conducting solar radiation studies and investigations. This is primarily attributed to its crucial role in computing radiative fluxes and heating rates at the surface, considering factors such as absorption, scattering, and emission of solar radiation by gases, aerosols, and clouds ( refer to Bartók et al. (2017); Yang et al. (2020). Moreover, the radiative scheme significantly influences the energy balance, temperature, precipitation, circulation, and overall variability of the climate system (Yang et al. 2020; Lu et al. 2023). Hence, the choice of the radiative scheme in a model is one of the essentials for improving the reliability of climate models. CMIP6 models adopted different methods and datasets to represent the solar or radiative components of the climate system, which varies among the models. For instance, in some models, total solar irradiance (TSI) or spectral solar irradiance (SSI) is used to prescribe solar forcing. SSI is responsible for the wave-length-dependent changes in solar radiation, which affects the stratospheric ozone chemistry and the different atmospheric layers (Matthes et al. 2017). Also, including or excluding solar-induced stratospheric ozone variations can modulate the solar forcing and impact the tropospheric climate. In addition, how aerosols interact with radiation, clouds, and chemistry can also affect the Earth's radiative balance by scattering and absorbing solar radiation, modifying cloud properties and precipitation, and altering atmospheric composition (Smith and Forster 2021). A brief description of the radiative processes in the selected CMIP6 models used in this study is presented in Table 1.

A subset of all the model data for solar radiation variable over Nigeria for the period $1990 - 2100$ is carried out in three climate epochs hereafter referred to as present-day climate (1990−2020), near-future (2020−2050), and far-future (2070−2100). All the models and ERA5 reference datasets were re-gridded to a common resolution of $0.25° \times 0.25°$ for comparison. We also calculated the projected change in solar radiation from the individual

**Table 1** Lists of CMIP6 models considered in this study and brief description of radiative transfer process

| S/N | Model name | Description | Horizontal resolution (lon × lat) |
|---|---|---|---|
| 1 | CAS-ESM2-0 (Chai 2020; Zhang et al. 2020) | Parametrizations for solar and thermal radiation through the atmosphere considered the absorption, emission, and scattering of radiation by gases, clouds, aerosols, and the Earth's surface. This allows for the representation of the energy balance between incoming solar radiation and outgoing longwave radiation Mlawer et al. (1997) | 1.4° x 1.4° |
| 2 | NorESM2-MM (Bentsen et al. 2019; Seland et al. 2020) | The two-stream Community Atmosphere Model version 4 (CAM4) scheme Iacono et al. (2008) includes short- and long-wave radiation processes, accounting for aerosols, clouds, ozone, water vapor, carbon dioxide and trace gases. Enhanced coefficients for water vapour absorption and updated solar constants improve radiative forcing and feedback accuracy. Briegleb (1992) | 1.25° × 0.94° |
| 3 | CIESM (Huang 2019; Lin et al. 2020) | A four-stream spherical harmonic expansion Zhang and Li (2013) approximation that reduces the error of radiative fluxes relative to the two-stream scheme in areas of large solar zenith angles during times when there is a thin optical depth of aerosol or clouds | 2.5° × 1.89° |
| 4 | EC-Earth3 (Döscher et al. 2021; EC-Earth 2019) | In EC-Earth, the IFS radiation scheme (specifically, the ecRad radiation scheme in cycle 43r3; (Hogan et al. 2017)) is utilized to calculate the optical properties for the 14 wavelength bands of the shortwave (SW) radiation. Specifically, the optical properties are computed at the band mean wavelengths and are weighted by the incoming solar radiation | 0.7° × 0.7° |
| 5 | EC-Earth3-CC (Döscher et al. 2021; EC-Earth 2021) | The same as EC-Earth3 | 0.7° × 0.7° |
| 6 | EC-Earth3-Veg (Döscher et al. 2021; EC-Earth 2019) | The same as EC-Earth3 | 0.7° × 0.7° |
| 7 | FGOALS-f3-L (He et al. 2019; Yu 2019) | The model adopted The Rapid Radiative Transfer Model for GCMs (RRTMG, (Clough et al. 2005)), which makes use of the correlated k-distribution approach as the primary radiation transfer employed in the model. This method accurately calculates the irradiance and heating rate over 16 longwave and 14 shortwave spectral intervals | 1.25° × 1° |
| 8 | BCC-CSM2-MR (Xin et al. 2018) | The model incorporates the radiative transfer scheme employed in CAM3 (Collins et al. 2004), while also considering the aerosol indirect effects | 1.12° × 1.12° |
| 9 | INM-CM5-0 (Volodin et al. 2017, 2019) | The model incorporates the parameterization of atmospheric radiation based on the work of (Galin 1998). It utilizes spectral transmission functions and employs the delta-Eddington approximation to accurately consider the absorption and scattering of radiation in the atmosphere caused by atmospheric gases, aerosols, and clouds | 2.0° × 1.5° |
| 10 | AWI-CM-1-1-MR (Song et al. 2019) | It uses the radiative scheme in the Max Planck Institution atmospheric model ECHAM 6.3 to calculate the short-wave and long-wave radiative fluxes at the top of the atmosphere, the surface, and each atmospheric level. The radiation scheme uses a two-stream approximation and a correlated-k method to compute the radiative transfer (Iacono et al. 2008) | 0.93° × 0.93° |

**Table 1** (continued)

| S/N | Model name | Description | Horizontal resolution (lon × lat) |
|---|---|---|---|
| 11 | FIO-ESM-2-0 (Bao et al. 2020; Song et al. 2019) | The model incorporates the radiative fluxes implemented in the Community Atmosphere Model version 5 (CAM5; (Neale et al. 2010)) for accurate calculations. Radiative fluxes and heating rates are computed using the RRTMG (Rapid Radiative Transfer Model for General Circulation Models) approach developed by (Iacono et al. 2008). RRTMG divides the solar spectrum into 14 shortwave bands and the infrared spectrum into 16 longwave bands. The model utilizes a two-stream delta-Eddington approximation, assuming homogeneously mixed layers, to account for both absorption and scattering in the determination of reflectance and transmittance. Furthermore, the shortwave radiation is calculated by RRTMG only when the cosine of the zenith angle is greater than zero, indicating that the sun is above the horizon | 1.25° × 0.94° |
| 12 | MPI-ESM1-2-HR (von Storch et al. 2017) | The model employs the radiative scheme ((Iacono et al. 2008)) from the Max Planck Institute atmospheric model ECHAM 6.3 to compute the shortwave and longwave radiative fluxes at various levels, including the top of the atmosphere, the surface, and each atmospheric level | 0.94° × 0.94° |
| 13 | CMCC-CM2-SR5 (Lovato and Peano 2020; Cherchi et al. 2019) | The model incorporates the radiative fluxes implemented in Community Atmosphere Model version 5 (CAM5; (Neale et al. 2010)) in which radiative fluxes and heating rates are computed using the RRTMG (Rapid Radiative Transfer Model for General Circulation Models) approach developed by (Iacono et al. 2008) | 1° × 1° |
| 14 | CMCC-ESM2 (Lovato et al. 2021, 2022; Cherchi et al. 2019) | The same as CMCC-CM2-SR5 | 0.9° × 1.25° |
| 15 | TaiESM1 (Lee and Liang 2020; Lee et al. 2020) | The radiative fluxes and heating rates within the atmosphere model CAM5 employs the Rapid Radiative Transfer Model for GCMs (RRTMG) introduced described in (Iacono et al. 2008) which incorporates a two-stream approximation, correlated k-distribution technique, and the Monte Carlo Independence Column Approximation method ((Pincus et al. 2003)). These techniques collectively contribute to accurately calculating the atmosphere's radiative properties and heating rates | 0.9° × 1.25° |
| 16 | MRI-ESM2-0 (Yukimoto et al. 2019a, b) | The radiative transfer process is based on MRI−CGCM3 (Yukimoto et al. 2012), which treats longwave (LW) and shortwave (SW) radiation separately. It calculates radiative flux in 9 LW bands and 22 SW bands, considering major absorptions by water vapour, carbon dioxide, and ozone in the 9.6 mm, visible, and ultraviolet bands. The SW scheme accounts for absorption by oxygen and Rayleigh scattering, while the LW scheme also includes additional gases (e.g. methane, dinitrogen monoxide, and chlorofluorocarbons) due to their greenhouse gas effects | 1.13° × 1.12° |

models in CORDEX RCMs, CMIP5 and CMIP6 GCMs relative to the present-day climate for RCP4.5 and SSP545 climate scenarios. The area averages along the different climatic zones of Nigeria were also considered and analyzed. The zones are as follows: Rainforest or Forest ($6.80°N$–$9.08°N$ and $2.79°E$–$12.08^{o}E$;), Guinea Savanna ($9.29°N$–$11.22°N$ and $3.71°E$–$12.77°E$), Coastal ($4.33°N$–$6.45°N$ and $4.41°E$–$8.86°E$) and Sahel ($11.62°N$–$13.15°N$ and $4.17°E$–$13.21°E$) as depicted in Fig. 1.

**Table 2** Lists of CMIP5 models considered in this study with their respective institutions, resolutions

| S/N | Model (References) | Institution | Horizontal resolution (lon × lat) |
|---|---|---|---|
| 1 | GISS-E2-H-CC (Schmidt et al. 2014) | National aeronautics and space administration, Goddard Institute for Space Studies | 2° × 2.5° |
| 2 | GISS-E2-R-CC (Schmidt et al. 2014) | National aeronautics and space administration, Goddard Institute for Space Studies | 2° × 2.5° |
| 3 | IPSL-CM5B-LR (Dufresne et al. 2013) | Institut Pierre-Simon laplace. | 1.9° × 3.75° |
| 4 | IPSL-CM5A-MR (Dufresne et al. 2013) | Institut Pierre-Simon laplace. | 1.25° × 2.5° |
| 5 | IPSL-CM5A-LR (Dufresne et al. 2013) | Institut Pierre-Simon laplace | 1.9° × 3.75° |
| 6 | FIO-ESM (Qiao et al. 2013) | First Institute of Oceanography (FIO) and Qingdao National Laboratory for Marine Science and Technology (QNLM), Qingdao, China | 2.5° × 2.0° |
| 7 | GFDL-ESM2MG (Donner et al. 2011) | NOAA Geophysical Fluid Dynamics Laboratory, USA | 2.0° × 2.0° |
| 8 | GFDL-ESM2M (Donner et al. 2011) | NOAA Geophysical fluid dynamics laboratory, USA | 2.0° × 2.0° |
| 9 | CNRM-CM5 (Voldoire et al. 2013) | Centre Européen et de Formation avancée en calcul Scientifique, National Center for Meteorological Research (CNRM-CERFACS), France | 1.4° × 1.4° |
| 10 | INMCM4 (Volodin et al. 2010) | Institute for Numerical Mathematics, Russia | 2.0° × 1.5° |
| 11 | MPI-ESM-MR (Zanchettin et al. 2013) | Max Planck Institute for Meteorology (MPI-M) | 1.875° × 1.85° |
| 12 | BNU-ESM (Ji et al. 2014) | College of Global Change and Earth System Science, Beijing Normal University China | 2.81° × 2.81° |
| 13 | ACCESS1-3 (Dix et al. 2013) | Commonwealth Scientific and Industrial Research Organization (CSIRO), Australia and Bureau of Meteorology (BOM), Australia | 1.875° × 1.25° |
| 14 | ACCESS1-0 (Bi et al. 2013) | Commonwealth Scientific and Industrial Research Organization (CSIRO), Australia and Bureau of Meteorology (BOM), Australia | 1.875° × 1.25° |
| 15 | CESM1-BGC (Long et al. 2013) | National Science Foundation, Department of Energy, National Center for Atmospheric Research USA | 1.25° × 0.94° |

**Table 3** Lists of CORDEX Models at 0.44° resolution used in this study

| S/N | RCM | References | Institution | Driving GCM(s) | Abbreviation |
|---|---|---|---|---|---|
| 1 | CLMcom-CCLM4-8-17 | (Panitz et al. 2015) | Climate Limited-area Modelling Community | CNRM-CM5; MOHC-HadGEM2-ES; MPI-M-MPI-ESM-LR | CCLM-CNRM; CCLM-HAD; CCLM-MPI |
| 2 | SMHI-RCA4 | (Meteorological 2017) | Swedish Meteorological and Hydrological Institute, Rossby Centre | CSIRO-Mk3-6-0; CERFACS-CNRM; IPSL-CM5A-MR; MIROC-MIROC5; HadGEM2-ES; M-MPI-ESM-LR; CCCma-CanESM2; NCC-NorESM1-M; NOAA-GFDL-ESM2M | RCA4-CSIRO; RCA4-CNRM; RCA4-CM5A; RCA4-MIROC5; RCA4-HAD; RCA4-MPI; RCA4-CanESM2; RCA4-NorESM; RCA4-GFDL |
| 3 | KNMI-RACMO22T | (KNMI 2017) | Royal Netherlands Meteorological Institute, De Bilt, The Netherlands | ICHEC-EC-EARTH; MOHC-HadGEM2-ES | RACMO-ICHEC; RACMO-HAD |
| 4 | MPI-CSC-REMO2009 | (GERICS 2017) | Helmholtz-Zentrum Geesthacht, Climate Service Center, Max Planck Institute for Meteorology | MPI-M-MPI-ESM-LR | REMO-MPI |

## Relative performance of CORDEX, CMIP5 and CMIP6 GCMs

Multi-model ensembles (MMEs) of CORDEX RCMs, CMIP5 and CMIP6 GCMs were obtained by a simple averaging method. The performance of the MMEs for CORDEX, CMIP5 and CMIP6 were compared to show their relative performance against the reference observation dataset across the different vegetation zones. The evaluation focused on assessing their ability to accurately replicate the monthly

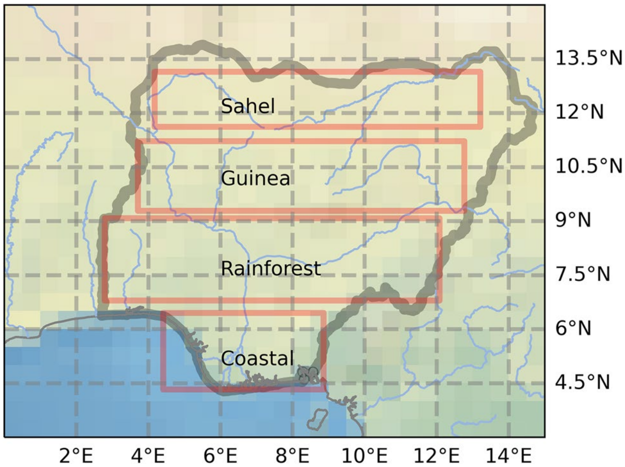


**Fig. 1** Map of the study area showing the different climatic zones analyzed

variations and inter-annual variability in solar radiation climatology within Nigeria during the time span from 1990 to 2020. Hence, the monthly variation of solar radiation from the MMEs for the different zones is investigated. We proceeded by considering the error measure for the MMEs relative to ERA5 by analyzing the mean bias and root mean square deviation across the different zones according to equations 1 and 2

$$MBE = \frac{1}{N}\sum_{i=1}^{N} MMEs^{i} - ERA5^{i} \tag{1}$$

This gives the direction of error as either positive or negative. Positive values of MBE show an overestimation of the model, while negative values indicate an underestimation.

Another error measure considered in this study is the root mean square deviation (RMSD). This measures the differences between the model's values and that observed from the reference observation data. A lower RMSD indicates good performance of the model with respect to the reference data.

$$RMSD = \sqrt{\frac{1}{N}\sum_{i=1}^{N}(MMEs^{i} - ERA5^{i})^{2}} \tag{2}$$

Taylor diagram (Taylor 2001) was also used to depict the relative performance of the individual models in CORDEX, CMIP5 and CMIP6. The Taylor diagram gives the statistical summary of the degree of correlation (SCC: spatial correlation coefficient (SCC)) between each of the models and ERA5, the root-mean-square deviation (RMSD), and the spatial standard deviation (SD). Hence, a concise comparison of the model's performance is also presented.

The numerical models' performance and evaluation were assessed with ERA5 reanalysis as reference data using time series and statistical analysis. The statistical analysis gives the performance of each model relative to ERA5 for the biases, correlation coefficient, standard deviation, and root mean square errors. On the other hand, the time series analysis is based on a comparison of ERA5 with the ensemble mean of model simulations from CORDEX, CMIP5, and CMIP6 experiments.

## Results and discussion

### Validation of models

Figure 2 shows the statistics of the monthly variation of solar radiation (SSRD) from ERA5 and the multi-model ensemble mean (MMEs) of SSRD from CMIP5, CMIP6, and CORDEX models across the four climatic zones of Nigeria from 1990 – 2020. The box-and-whisker plots demonstrate the dispersion of the SSRD from the MMEs and ERA5, offering valuable insights into the level of agreement among the data. In the box-and-whisker plots, the lower quartile (25th percentile) is represented by the lower part of the box and whisker, while the median (50th percentile) is denoted by the line dividing the box. The upper quartile (75th percentile) is depicted by the upper part of the box. The interquartile range, which indicates the data variability within the middle 50% of the observations, is calculated as the difference between the upper and lower quartiles. The data points that lie outside the whiskers of the box plot, identified by dark-filled triangles, are referred to as outliers. These outliers represent data values that are significantly distant from the rest of the data in numerical terms. It has been established that the degree of variability and heterogeneity among the data sources increases with the size of the box and the distance between the whiskers (Zhou et al. 2021). Therefore, the data distribution is positively skewed if the whisker length at the higher quartile is longer than that at the lower quartile and vice versa (Wang et al. 2018).

In contrast to CMIP5 and CORDEX SSRD, greater similarities exist between ERA5 and CMIP6 in the Coastal and Forest zones. Also, considering the characteristics of the boxplots, similarities between ERA5 and CMIP6 are more pronounced during the dry season (December, January and February). Specifically, for the CMIP5 and CORDEX, modelled solar radiation distributions across the entire zones are relatively the same for all the months. This can be associated with the CORDEX RCMS downscaling some CMIP5 GCMs. It is also apparent that during the dry season, the lower quartile whisker lengths from CMIP5 were longer than those from CORDEX but vice-versa during the rainy season (March to October). This suggests that generally higher solar radiation variability is modelled by CMIP5 during the dry season, while CORDEX data shows the highest variability

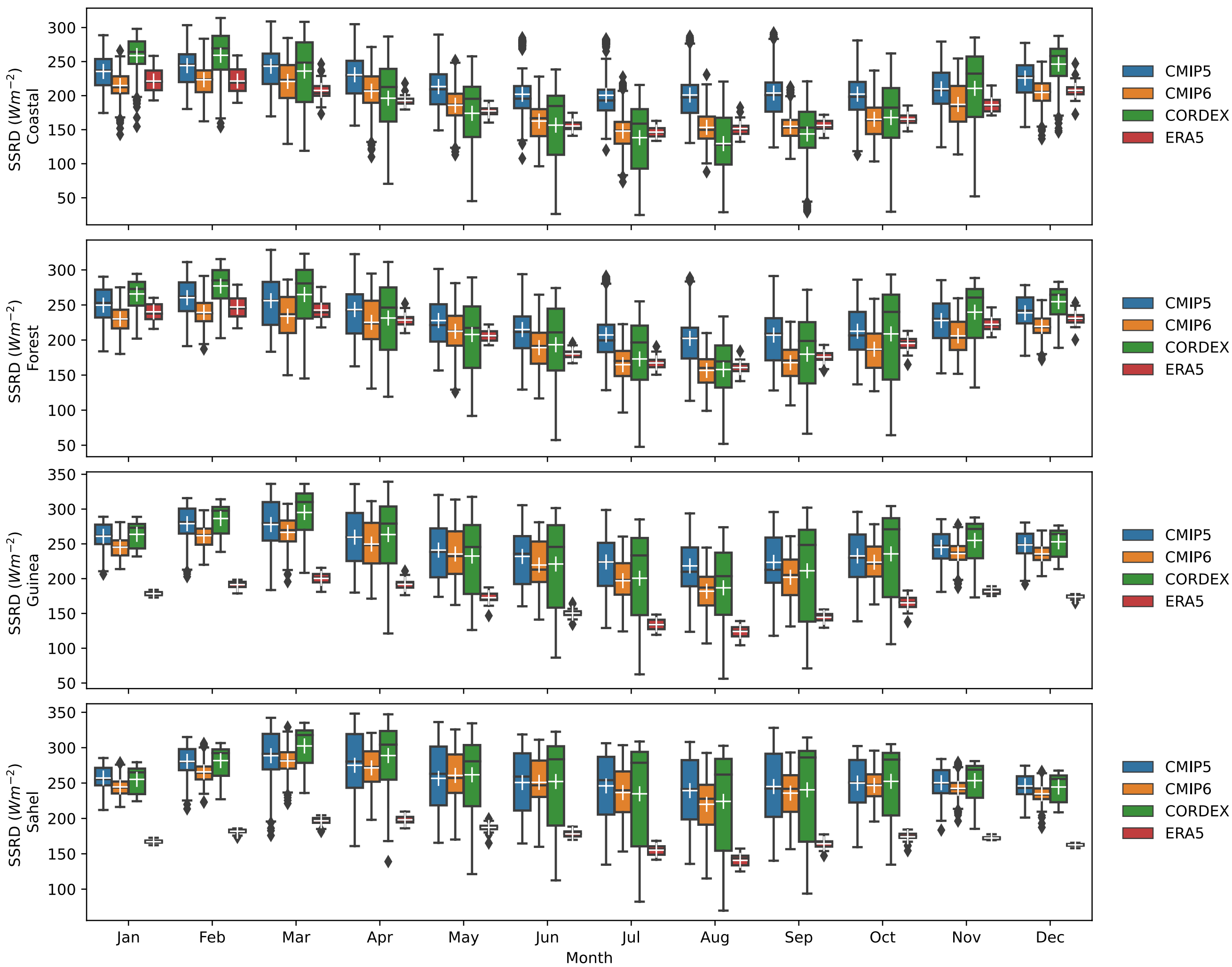


**Fig. 2** Monthly variation of solar radiation across different climatic/vegetation zones of Nigeria from ERA5 and ensembles of CMIP5, CMIP6 and CORDEX averaged over 1990–2020

during the rainy season. It can also be observed that CMIP5 and CORDEX models have the most pronounced negative skewness in their distributions, unlike ERA5 and CMIP6, which show nearly symmetry distributions. However, it was found that in the Guinea and Sahelian zones, the differences between the ERA5 SSRD and simulated SSRDs from CMIP5, CMIP6, and CORDEX multi-models ensemble means were quite large, resulting in lesser values for the ERA5 SSRD than for the simulated models. The increased attenuating effects of aerosols, cloudiness, and humidity which are of paramount significance in these zones on solar radiation make it difficult for regional climate models to replicate across these zones. This may account for the disparities between ERA5 SSRD and simulated SSRDs from CMIP5, CMIP6, and CORDEX models (Tang et al. 2021; Ojo et al. 2021). For instance in the Sahel, dust aerosols from the Sahara desert are common, and they can lead to substantial reductions in solar radiation during certain periods. Hence, accurate representation of aerosols in climate models is essential for realistic solar radiation simulations. Generally, solar radiation values during the dry season are higher than in the wet season. The ability of the different models to capture this trend is important for agricultural, health, and energy considerations. From our results, the models captured the seasonal pattern of solar radiation in both Coastal and Forest zones but performed poorly by grossly overestimating for the Guinea and Sahel. A similar country-scale study ((Patchali et al. 2020) also reported similar model overestimations relative to the reference observation data. The differences between the performances can be attributed to the parameterization of cloud cover between coastal and inland regions Chakraborty and Lee (2021). This suggests the need to bias-correct the solar radiation data for the Guinea and Sahel zone to provide reliable estimates.

Figure 3 shows the biases between solar radiation from ERA5 and the 16 CIMP5, CIMP6, and 15 CORDEX models

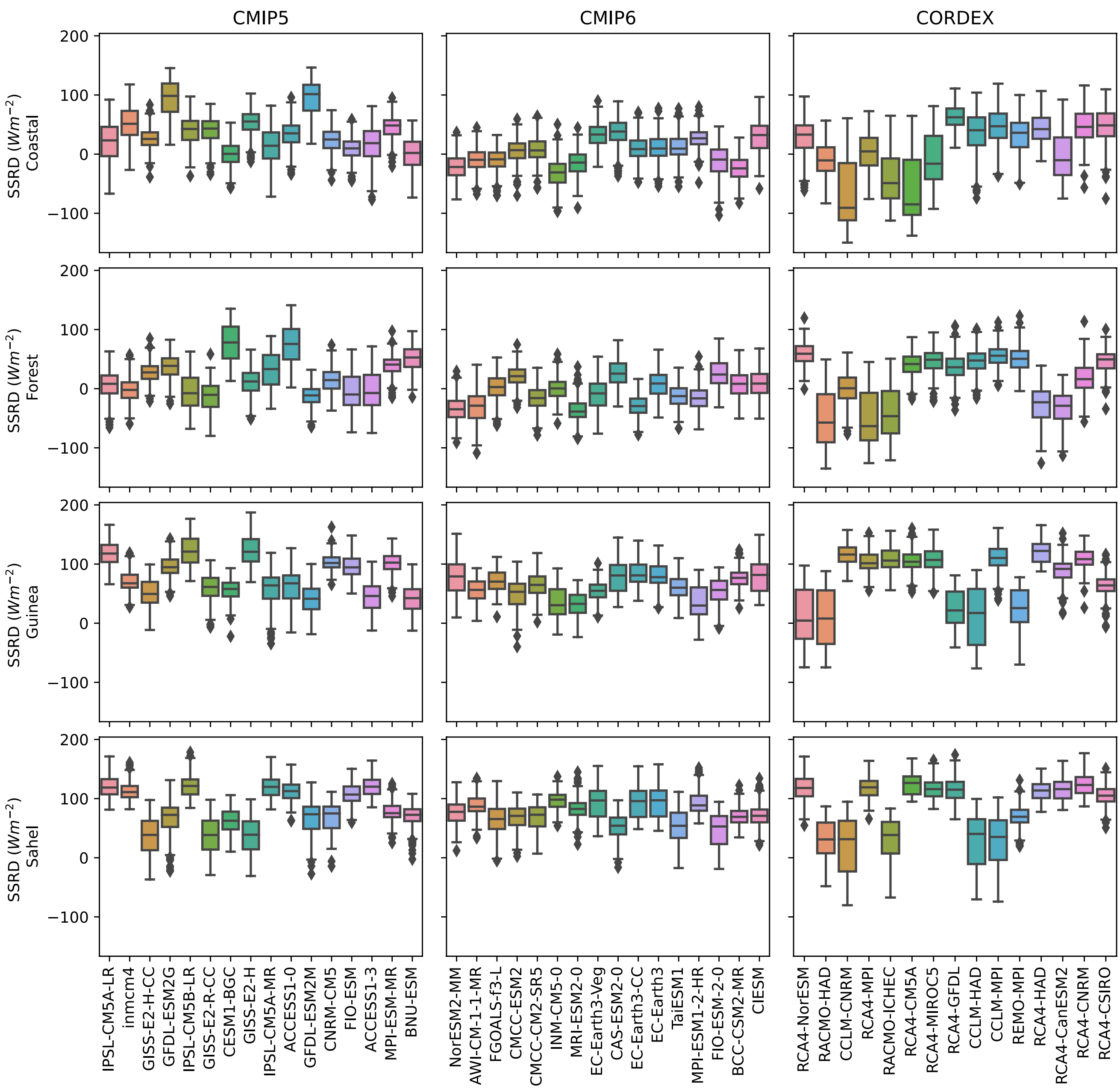


**Fig. 3** CORDEX, CMIP5, CMIP6 models mean biases relative to ERA5 for solar radiation in different climatic zones of Nigeria averaged for 1990–2020

across the four climatic zones in Nigeria. The essence is to see the models' performances across Nigeria's four climatic zones. A general outlook of Fig. 3 shows that all CMIP6 models consistently exhibit the lowest bias across the Coastal and Forest zones for all months compared to CMIP5 and CORDEX. The increased resolution and physics configuration of CORDEX models does not necessarily translates to improve performance of solar radiation simulation across the different vegetation zones of Nigeria compared to the CMIP5 models. Generally, most of the CMIP5 and CORDEX models overestimated solar radiation across each of the zones by up to 100 W $m^{-2}$. By standard, the model with the lowest mean bias is considered to have performed accurately above others, although the ideal desirable value for the bias is zero.

Considering the mean bias values indicated by the midlines of boxplots in the figure, the best-performed model can be proposed for each zone by category. In the CIMP5 category, the Coastal zone exhibited the lowest mean bias with the CESM1-BGC GCM, while the Forest zone showed the lowest mean bias with the inmCM4 GCM. In the Guinea zone, the GFDL-ESM2M model had the lowest mean bias, and in the Sahelian zone, the GISS-E2-H-CC model showed the lowest mean bias. Moving to the CIMP6 GCMs, the Coastal zone showed the lowest mean bias with the FIO-ESM-2-0 and INM-CM5-0 models, while the Forest zone had the lowest mean bias with the MRI-ESM2-0 GCM. The Guinea Savannah zone exhibited the lowest mean bias with the MPI-ESM1-2-HR model, while the Sahelian zone showed the lowest mean bias with the TAiESM1 model. With the CORDEX RCMs, the Coastal zone indicated the lowest mean bias with the CCLM-CNRM model, while the Forest zone displayed the lowest mean bias with the RCA4-MPI model. The Guinea Savannah zone showed the lowest mean bias with the RCA4-NorESM model, and the Sahelian zone had the lowest mean bias with RACMO-HAD and CCLM-CNRM models.

Previous studies which showed similar biases attributed it to the underestimation of anthropogenic aerosols Wang et al. (2022), increasing atmospheric absorption in line with the increase of water vapor content Bartók et al. (2017), or cloud phase and vertical structure representations Cesana et al. (2022). Within the Sahel and Guinea region, the predominant aerosol source is the natural dust from the Bodele region. However, anthropogenic sources are also predominant but not usually accounted for. Hence, the underestimation of the anthropogenic sources could be responsible for the poor performance of the models in the regions.

Figure 4 shows the inter-annual monthly solar radiation variability in Nigeria's four climatic zones, as observed by ERA5 and simulated by MMEs of CIMP5, CIMP6, and CORDEX models from 1990 to 2020. The figure reveals consistent seasonal and non-stationary patterns across the MMes of the models, recurring every 12 months along the Coastal and Forest zones. Across these two zones, the MMEs of the model exhibit similar pattern for the inter-annual monthly variability during 1990 – 2020. Although the MMEs of the model grossly overestimate the magnitude of the solar radiation by about 50 W $m^{-2}$ in the Sahel and Guinea zones, the pattern are reasonably well reproduced by the model's MMEs. However, CIMP5 exhibited the largest magnitude of differences from the reference ERA5 data in all the climatic zones. This large disparity has obviously been corrected in CIMP6, thus making CMIP6 better align solar radiation from ERA5 in these zones.

These results demonstrated relatively great performance of the models in the representation of the inter-annual variations along the coastal and forest zones, that closely align

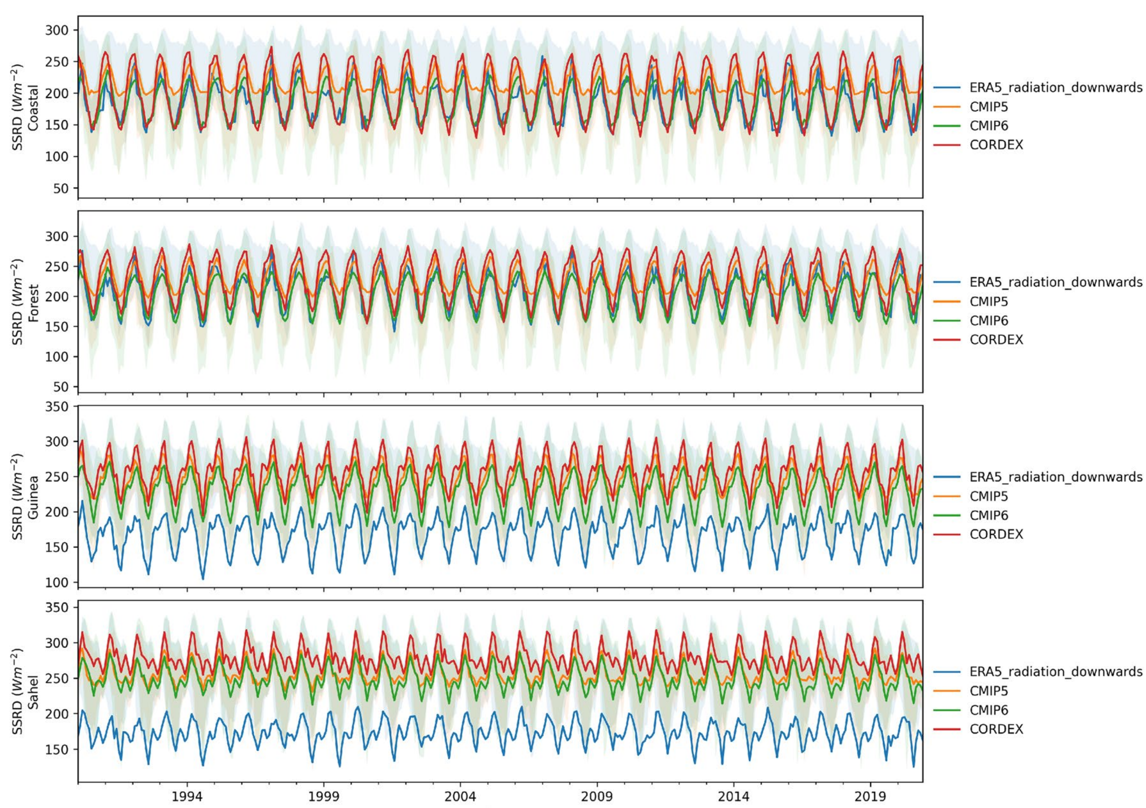


**Fig. 4** Inter-annual monthly variability of solar radiation based on ERA5, and ensemble mean of CMIP5, CMIP6, and CORDEX from 1990–2020

with ERA5. However, in the Guinea and Sahel regions, there were consistent instances of overestimation of the inter-annual variations, potentially resulting from various contributing factors that warrant further investigation. To ensure data accuracy for local research, bias correction of model simulation of solar radiation should be adopted for Guinea and Sahel zones. Inter-annual solar radiation variations promise insights into long-term influences and drivers affecting the climate.

Figure 5, 6, 7 depicts Taylor's Diagrams for the CIMP5, CIMP6, and CORDEX models simulation of SSRD with reference to ERA5. Taylor diagrams are capable of giving the preciseness of different models in comparison with observations using the three combined statistical parameters, including correlation coefficient (CC), standard deviation (SD), and root mean square errors (RMSD) with a series of points on a polar plot (Solomon 2007; Taylor 2001). The best model is selected based on the closer distance from the reference data point on the diagram's horizontal axis in addition to the highest value of CC and lowest values of SD and RMSD (Heo et al. 2014). Therefore, from Fig. 5, the best-performed models for CIMP5 were ACCESS-0 and IPSL-CM5B-LR (0.86) in the Coastal zone; IPSL-CM5B-LR (0.89) in the Forest zone; GISS-E2-R-CC, BNU-ESM, and CESM1-BGC (0.87) in the Guinea zone; and BNU-ESM (0.77) in the Sahel zone. Also, from Fig. 6, the best-performed models for CIMP6 were MPI-ESM1-2-HR and BCC-CSM2-MR (0.84) in the Coastal zone; EC-Earth3-CC (0.89) in the Forest zone; FGOALS-f3-L and CMCC-CM2-SR5 (0.88) in the Guinea zone; and INM-CM5-0 (0.82) in the Sahelian zone. Meanwhile, from Fig. 7, the best-performed models for CORDEX wereRCA4-CM5A (0.87) in the Coastal zone; CCLM-HAD (0.91) in the Forest zone, CCLM-HAD (0.91) in the Guinea zone and also CCLM-HAD (0.76) in the Sahel zone. It is worthy of note that 64.06% of the CIMP5 models, 95.3% of the CIMP6 models, and 98.4% of the CORDEX model had correlation coefficients > 0.5 across the four climatic regions in Nigeria.

## Projection of solar radiation under different scenarios

Figures 8 to 9 provide valuable insights into the future projections of solar radiation across Nigeria's four climatic zones, based on simulations from CIMP5, CIMP6, and CORDEX models under different emissions scenarios

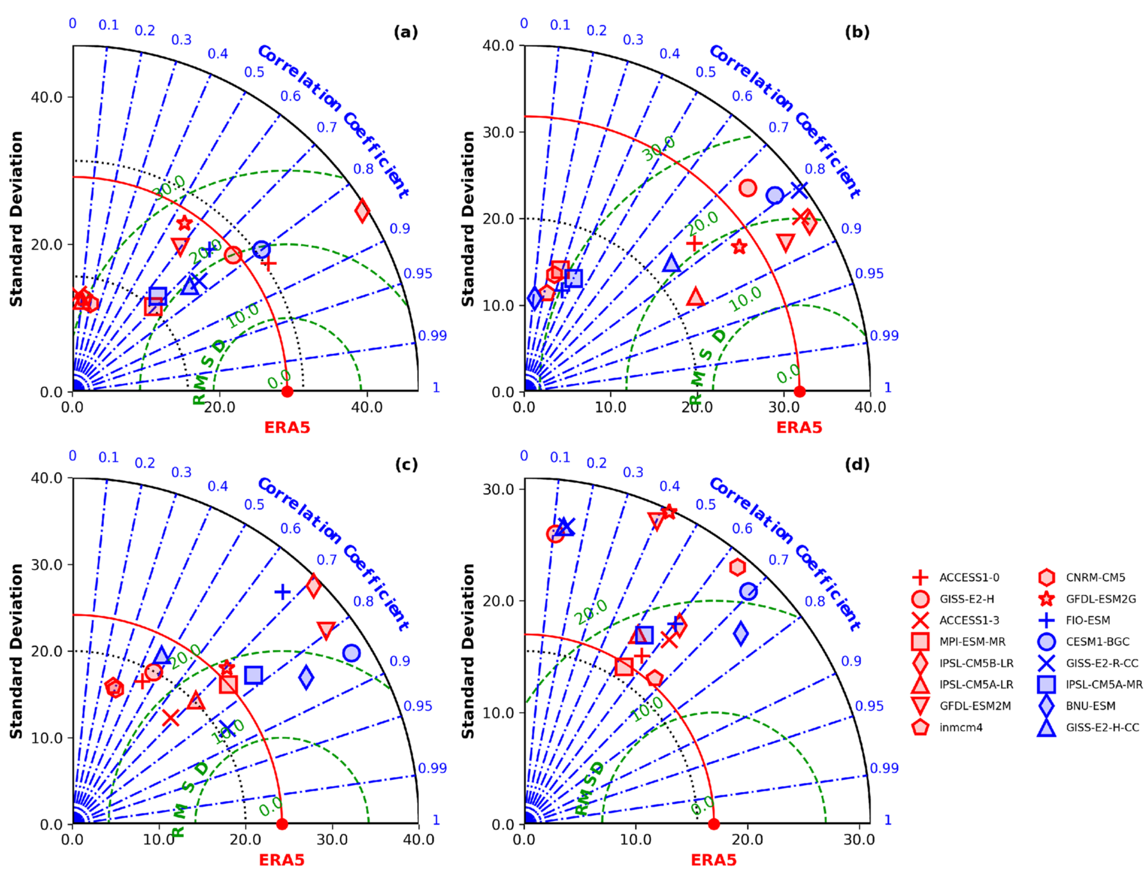


**Fig. 5** Taylor diagram of CIMP5 models along the **a** Coastal, **b** Forest, **c** Guinea, and **d** Sahel for the period 1990−2020

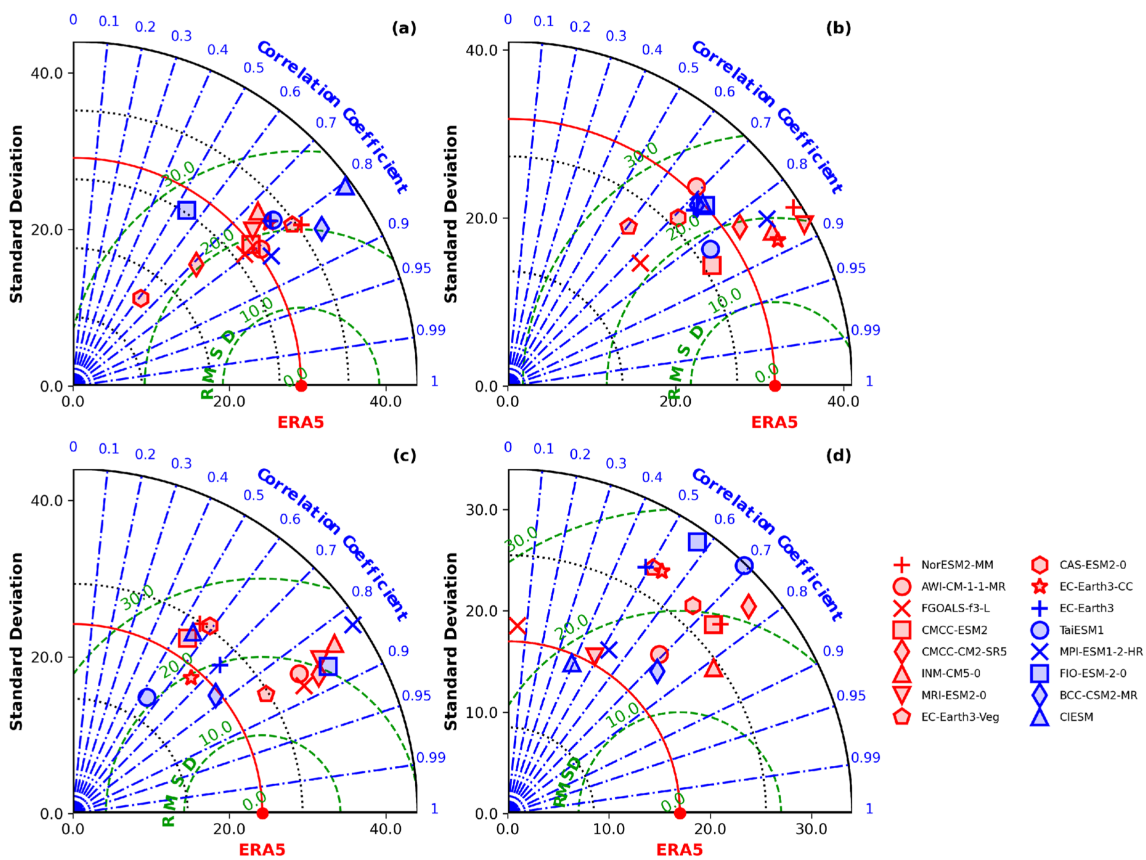


**Fig. 6** Taylor diagram of CIMP6 models along the **a** Coastal, **b** Forest, **c** Guinea, and **d** Sahel 1990−2020

(RCP4.5/SSP5−4.5 and RCP8.5/SSP5−8.5) for the mid-future (2020−2050) and far-future (2070−2100).

### Coastal zone

In the Coastal zone (Fig. 8), the majority of CMIP5, CMIP6, and CORDEX models projected solar dimming (negative projection changes) of more than 80%, 92%, and 60%, respectively, under RCP4.5/SSP−4.5 scenarios. This remarkable agreement among the models suggests a robust projection of solar dimming in this region. The magnitude of projected solar radiation changes varies, with CMIP6 models showing the highest dimming at $-6W/m^2$, and CMIP5 models indicating the lowest dimming at $-0.5W/m^2$. In the far-future, there is still considerable agreement among more than 50dimming in the Coastal zone under RCP4.5/SSP−4.5 scenarios, whereas CMIP6 models show agreement with only 50% of the models. The magnitude of solar brightening varies, with CMIP6 models projecting the highest brightening at $+11W/m^2$, and the lowest at $+5W/m^2$. Under RCP8.5/SSP5−8.5 scenarios (Fig. 9) for the mid-future, the models consistently project solar dimming in the Coastal zone, with 81% of CMIP5, 93% of CMIP6, and 60% of CORDEX models indicating dimming. The magnitude of dimming ranges from $-12W/m^2$ (highest) in CMIP5 models to $-1W/m^2$ (lowest) in CORDEX models. Also, in the far-future under RCP8.5/SSP5−8.5 scenarios, there is strong agreement among 87CMIP6, and 73% of CORDEX models regarding solar dimming in the Coastal zone, with the highest magnitude of dimming projected at $-35W/m^2$ from CMIP6 models. Overall, the results indicate a consistent projection of solar dimming in the Coastal zone across different emissions scenarios and time periods, with some variations in magnitude among the models. These findings highlight the importance of considering different climate models in understanding future solar radiation changes and their potential impacts on the region's climate and environment.

### Forest zone

In the Forest zone, for the mid-future under the RCP4.5/SSP5−4.5 scenario (Fig. 8), a considerable proportion of CMIP5 (75%), CMIP6 (87%), and CORDEX (60%) models project solar dimming. The highest magnitude of projected solar dimming is $-8W/m^2$ from CMIP6 models, while the lowest dimming values are $-1W/m^2$ from both CMIP5 and CORDEX models. Looking further into the far-future, approximately 50% of the models from CMIP5, CMIP6, and

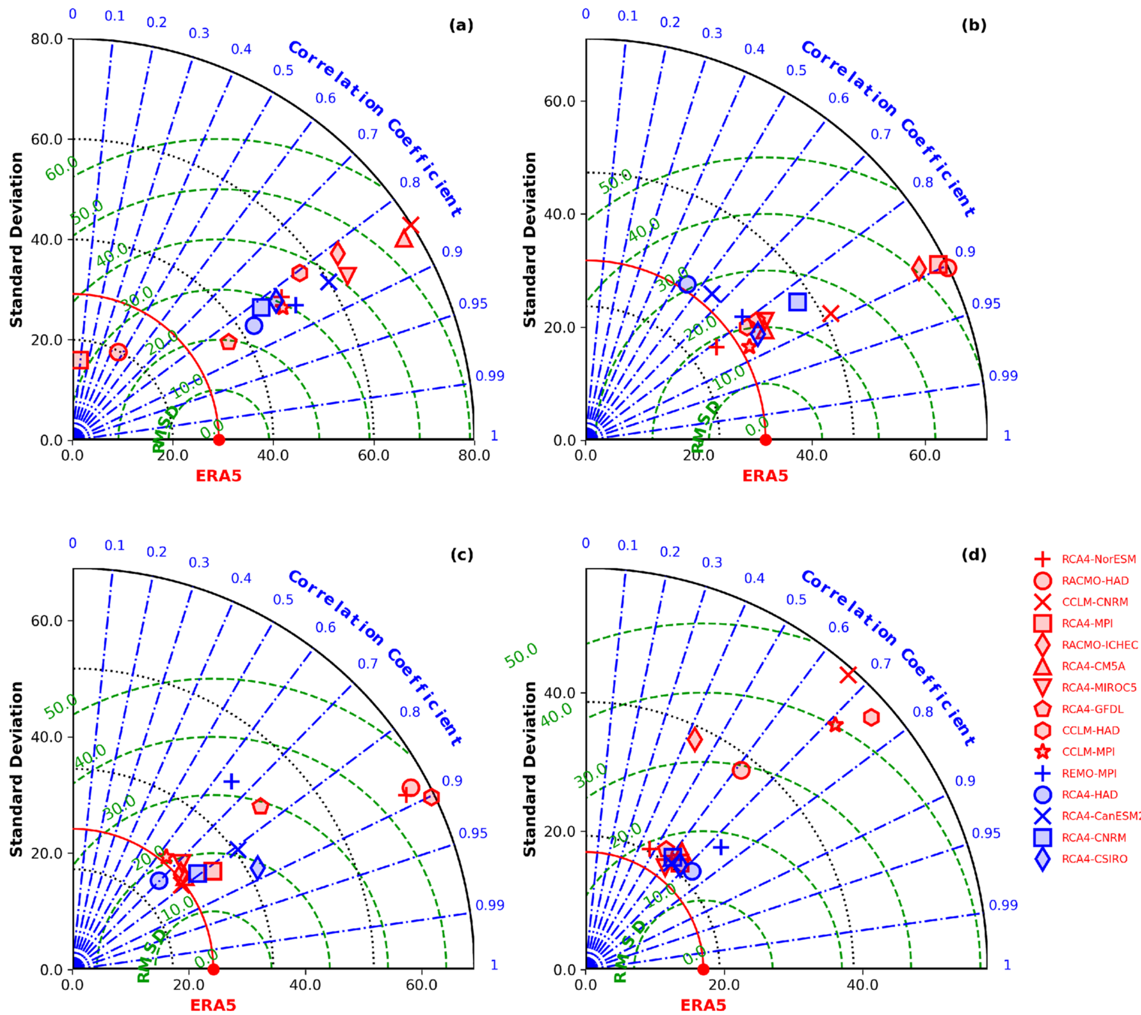


**Fig. 7** Taylor diagram of CORDEX models along the **a** Coastal, **b** Forest, **c** Guinea, and **d** Sahel 1990–2020

CORDEX project both solar dimming and solar brightening. The highest magnitude of solar dimming is projected at $-8W/m^2$, while the highest magnitude of solar brightening is projected at $10W/m^2$. On the other hand, the lowest magnitude of solar dimming is $-1W/m^2$, while the lowest magnitude of solar brightening is $0.6W/m^2$. Under RCP8.5/SSP5−8.5 scenario (Fig. 9), 87CMIP5, 75% of CMIP6 and more than 60 % of CORDEX strongly agrees on the projected solar dimming in the mid-future and far-future for the forest zone. However, the magnitude of the projected dimming is largest with the CMIP6 models with magnitude that is up to $-35W/m^2$. The lowest projected dimming is within the range of $-1W/m^2$ and $-5W/m^2$ in both CORDEX and CMIP5 models. These results also suggest significant variations in solar radiation projected changes among the different models and scenarios, emphasizing the complexity of projecting future solar radiation patterns in the Forest zone. The importance of further research to understand the underlying drivers and mechanisms responsible for these projected changes is crucial. This will also improve the accuracy of climate models in simulating solar radiation dynamics.

## Guinea zone

In the Guinea zone, all the models consistently project solar dimming during the mid-future under the RCP4.5/SSP5−4.5 scenario (Fig. 8), with CMIP6 models exhibiting the highest magnitude of $-12W/m^2$. This unanimity in dimming signals suggests a robust projection among the models for this period. However, in the far-future, there is notable variation among the models regarding the projected change signal. Approximately 50 % of the models in CMIP5 and CORDEX show agreement on the direction of change, while only 40 % of CMIP6 models indicate a solar brightening in the far-future along the Guinea zone. The agreement observed between CORDEX and CMIP5 models can be attributed to the utilization of similar climate forcings, which might contribute to their aligned projections. Under the RCP8.5/

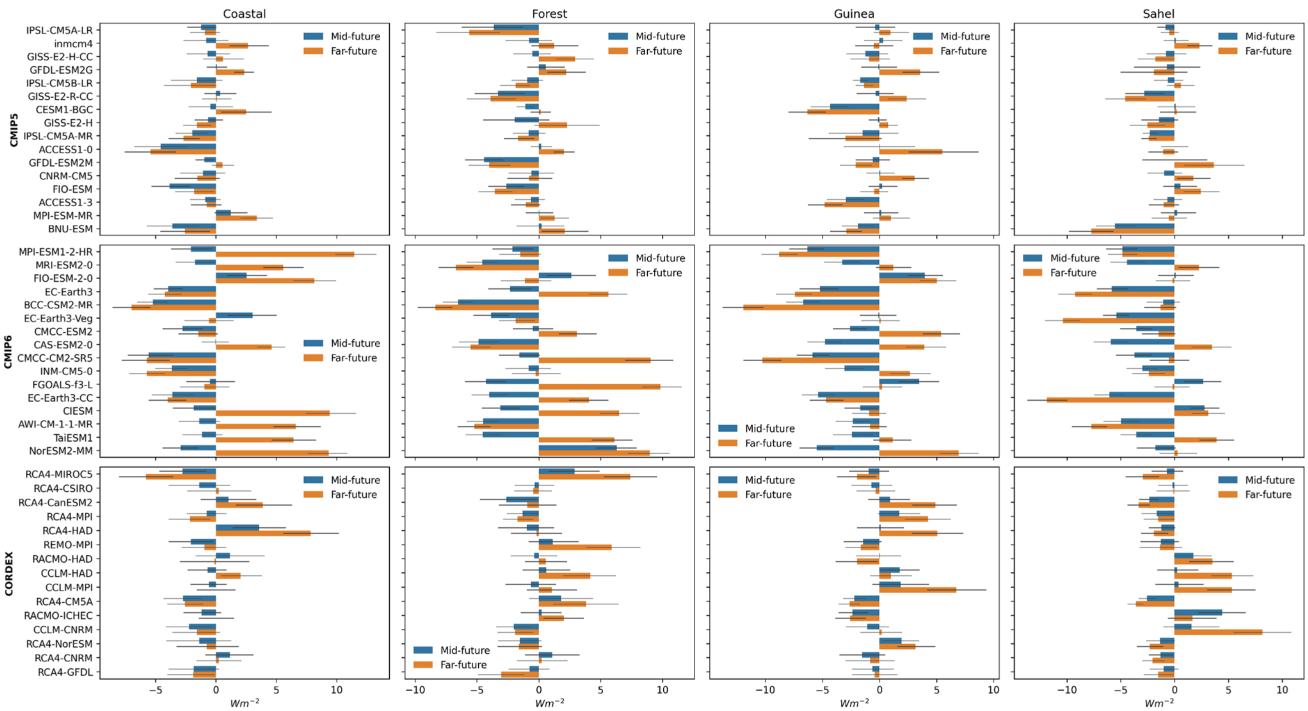


**Fig. 8** Projected changes in solar radiation under RCP4.5/SSP5−4.5 for the different climatic zones across Nigeria in the mid-future (2020-2050) and far-future (2070-2100)

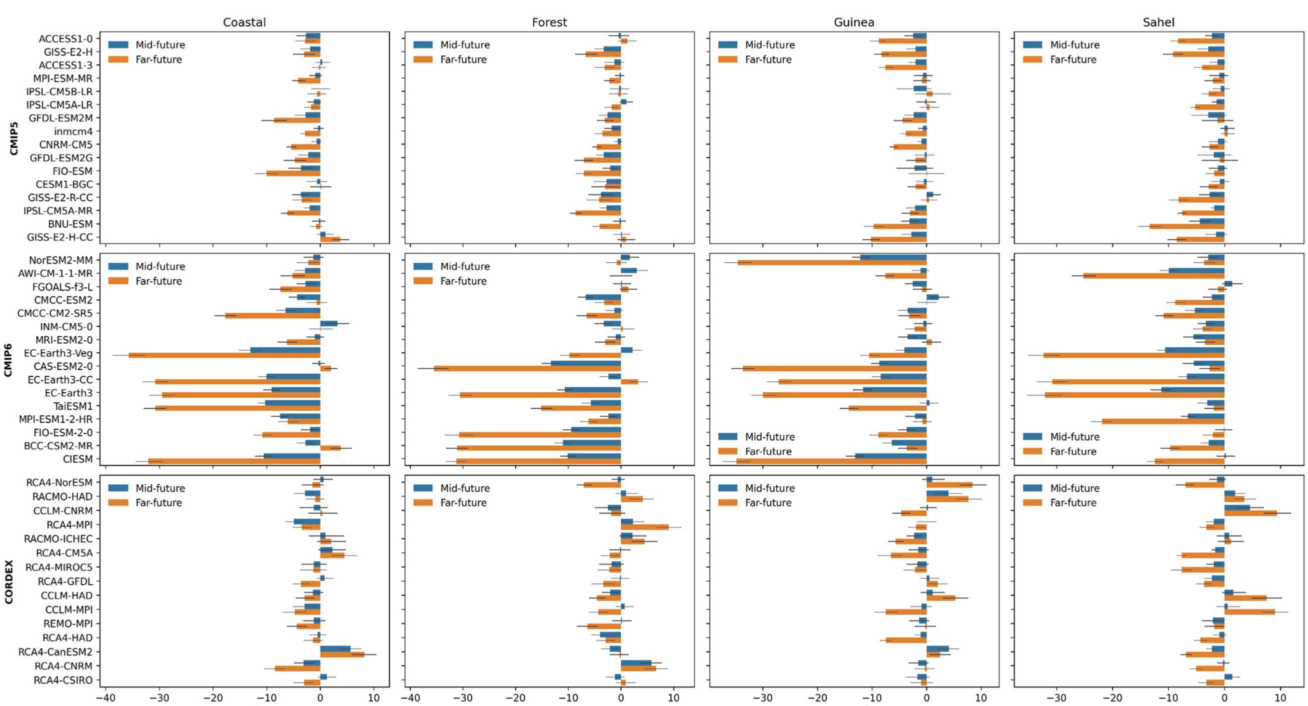


**Fig. 9** Projected changes under RCP8.5/SSP5−8.5 for the different climatic zones across Nigeria in the mid-future (2020-2050) and far-future (2070-2100)

SSP5−8.5 scenario (Fig. 9), more than 90% of CMIP5, 87 % of CMIP6, and 60% of CORDEX models project solar dimming for both the mid-future and far-future periods. The highest and lowest magnitudes of solar dimming in the mid-future and far-future are observed at $-12W/m^2$ and $-35W/m^2$, respectively. These results emphasize the consensus among the models in projecting solar dimming in the mid-future, providing confidence in the reliability of the projections. However, the varying signals in the far-future highlight the complexity and uncertainty involved in projecting future solar radiation changes in the Guinea zone.

### Sahel

Along the Sahel zone, a larger percentage (60−80%) of the models projected solar dimming under RCP4.5/SSP5−4.5 and RCP8.5/SSP5−8.5 scenarios. The largest projected change occur in the far-future of RCP8.5/SSP5−8.5 scenarios with a magnitude of $-35W/m^2$ compared to the $-12W/m^2$ from RCP4.5/SSP5−4.5 scenario.

Generally, the inferences from Figs. 8–9 showed that most of the models predicted solar dimming, that is, negative values of projected changes in solar radiation for both scenarios for the mid-and far-futures. The solar dimming in the mid-future is less than that of the far-future across the four climatic zones in agreement with (Wu et al. 2022). Solar radiation is critical to the ecosystem and economy of tropical countries. Globally, there is an increasing demand and move towards renewable energy with solar energy being the most accessible. The future of solar radiation within the country has a direct effect on available renewable energy in Nigeria. Most models projected a solar radiation dimming over different regions of the country. This projected dimming will reduce available solar radiation for power generation Jiang et al. (2023). There is the need for the country to consider mitigation and adaptation strategies such as co-locating solar power stations with wind and nuclear power stations to support the projected dimming, reduction of air pollution, and adoption of innovative energy storage systems. The dimming of solar radiation can also have impact on crop production. It has been reported that solar dimming affects maize production Meng et al. (2020). The impact of solar dimming can be reduced by cultivar improvement Liu et al. (2021).

## Conclusion

This study has shown the distribution of solar radiation across four climatic zones in Nigeria. These are the Forest, Guinea, Coastal, and Sahel zones. As expected, tropical regions generally have higher solar radiation than locations in higher-latitude. In contrast, renewable energy from solar radiation has been better maximized in higher latitudes than equatorial areas. However, as evidenced in this study, the higher solar radiation in tropical areas makes it suitable for solar energy potentials. For most emerging economies in West Africa, like Nigeria, there is so much hope in eradicating energy poverty if future solar radiation can be projected using available computing techniques and Earth Observation products. Solar radiation, in conjunction with temperature, drives the evaporation of water from the surface. This makes it an essential factor in the water cycle, indicating drought and agricultural productivity.

Solar radiation data challenges have been in the African tropics due to the high cost of equipment and maintenance. Alternative sources of data used in this region are satellite and numerical models. Understanding the efficiency of these models will help in making decisions. Hence, there is the need to first and foremost investigate the performance of reanalysis datasets compared with the numerical climate models for future climate projections of solar radiation in Africa. Beyond historical data, it is imperative to investigate future scenarios of solar radiation in the tropical region due to its socio-economic and environmental importance and relevance. This study's ERA5 reanalysis agrees with the CMIP6 simulated SSRD during the dry months (November to February) along the Coastal and Forest zones. Still, significant differences are found along the Guinea Savannah and Sahelian. This suggests that the effects of aerosols, cloudiness, and humidity on solar radiation must be well represented as this could cause the observed differences.

In the mid and far future, the models from the CORDEX, CMIP5, CMIP6 suggested solar dimming in all climatic zones under the SSP5−8.5 scenario. This is inferred as negative values of projected changes in solar radiation. Specifically, solar dimming in the mid-future is less than that of the far future across the four regions. In light of the changing climate, solar dimming has been attributed to increased aerosol particles due to pollution, dust, and other factors. These pollutants absorb solar energy and reflect the sunlight into space. Across most urban centres, these pollutants have also been responsible for cloud droplets. Hence, further studies still need to fully understand the role and dynamics of atmospheric pollutants and how they influence solar radiation intensity and dimming. The projected decrease in solar radiation across most models under the SSP5−8.5 scenario suggests the region needs to begin adaptation planning.

**Acknowledgements** We thank the Working Group on Coupled Modelling of the World Climate Research Programme for coordinating and promoting CMIP5, CMIP6 and CORDEX experiments. We thank the different modelling groups for their efforts in generating and sharing model outputs. In addition, the Earth System Grid Federation infrastructure, an international effort led by the U.S. Department of Energy's Program for Climate Model Diagnosis and Intercomparison, the European Network for Earth System Modelling and other partners in the Global Organisation for Earth System Science Portals (GO-ESSP) for archiving the data and facilitating access. Additionally, we acknowledge the support of the various funding agencies that contribute to CMIP5, CMIP6, CORDEX and ESGF.

**Funding** The authors did not receive any funding for this research.

**Availability of data and materials** All data used in this study are publicly available in repositories stated in the manuscript.

## Declarations

**Conflict of interest** The authors declare that there was no conflict of interest.

**Ethical approval** Not applicable.

**Consent to participate** Not applicable.

**Code availability** Authors can make the code available on reasonable requests.

## References

Avila N, Carvallo JP, Shaw B, Kammen DM (2017) The energy challenge in sub-saharan africa: a guide for advocates and policy makers. Gener Energy Sustain Equitable Dev Part 1:1–79

Babar B, Graversen R, Boström T (2019) Solar radiation estimation at high latitudes: assessment of the cmsaf databases, asr and era5. Sol Energy 182:397–411

Bao Y, Song Z, Qiao F (2020) Fio-esm version 2.0: model description and evaluation. J Geophy Res Oceans 125(6):2019–016036

Bartók B, Wild M, Folini D, Lüthi D, Kotlarski S, Schär C, Vautard R, Jerez S, Imecs Z (2017) Projected changes in surface solar radiation in cmip5 global climate models and in euro-cordex regional climate models for europe. Clim Dyn 49:2665–2683

Bentsen M, Oliviè DJL (2019) NCC NorESM2-MM model output prepared for CMIP6 CMIP historical. Earth Syst Grid Fed. https://doi.org/10.22033/ESGF/CMIP6.8040

Bi D, Dix M, Marsland S, O'Farrell S, Rashid H, Uotila P, Hirst A, Kowalczyk E, Golebiewski M, Sullivan A et al (2013) The access coupled model: description, control climate and evaluation. Aust Meteorol Oceanogr J 63(1):41–64

Briegleb BP (1992) Delta-eddington approximation for solar radiation in the ncar community climate model. J Geophys Res Atmos 97(D7):7603–7612

Cesana GV, Khadir T, Chepfer H, Chiriaco M (2022) Southern ocean solar reflection biases in cmip6 models linked to cloud phase and vertical structure representations. Geophys Res Lett 49(22):2022–099777

Chai Z (2020) CAS CAS-ESM2.0 model output prepared for CMIP6 CMIP. Earth Syst Grid Fed. https://doi.org/10.22033/ESGF/CMIP6.1944

Chakraborty T, Lee X (2021) Large differences in diffuse solar radiation among current-generation reanalysis and satellite-derived products. J Clim 34(16):6635–6650

Chanchangi YN, Adu F, Ghosh A, Sundaram S, Mallick TK (2022) Nigeria's energy review: focusing on solar energy potential and penetration. Environ Dev Sustain 25:5755

Cherchi A, Fogli PG, Lovato T, Peano D, Iovino D, Gualdi S, Masina S, Scoccimarro E, Materia S, Bellucci A et al (2019) Global mean climate and main patterns of variability in the cmcc-cm2 coupled model. J Adv Model Earth Syst 11(1):185–209

Clough S, Shephard M, Mlawer E, Delamere J, Iacono M, Cady-Pereira K, Boukabara S, Brown P (2005) Atmospheric radiative transfer modeling: a summary of the aer codes. J Quant Spectrosc Radiat Transfer 91(2):233–244

Collins WD, Rasch PJ, Boville BA, Hack JJ, McCaa JR, Williamson DL, Kiehl JT, Briegleb B, Bitz C, Lin S-J et al (2004) Description of the ncar community atmosphere model (cam 3.0). NCAR Tech Note NCAR/TN-464+ STR 226:1326–1334

Diaci J (1999) Solar radiation measurements in forests-i. evaluation of methods and instruments. Research Reports Forest and Wood Science and Technology, 105–138

Dix M, Vohralik P, Bi D, Rashid H, Marsland S, O'Farrell S, Uotila P, Hirst T, Kowalczyk E, Sullivan A et al (2013) The access coupled model: documentation of core cmip5 simulations and initial results. Aust Meteorol Oceanogr J 63(1):83–99

Donner LJ, Wyman BL, Hemler RS, Horowitz LW, Ming Y, Zhao M, Golaz J-C, Ginoux P, Lin S-J, Schwarzkopf MD et al (2011) The dynamical core, physical parameterizations, and basic simulation characteristics of the atmospheric component am3 of the gfdl global coupled model cm3. J Clim 24(13):3484–3519

Döscher R, Acosta M, Alessandri A, Anthoni P, Arneth A, Arsouze T, Bergmann T, Bernadello R, Bousetta S, Caron L-P et al (2021) The ec-earth3 earth system model for the climate model intercomparison project 6. Geosci Model Dev Discuss 2021:1–90

Dufresne J-L, Foujols M-A, Denvil S, Caubel A, Marti O, Aumont O, Balkanski Y, Bekki S, Bellenger H, Benshila R et al (2013) Climate change projections using the ipsl-cm5 earth system model: from cmip3 to cmip5. Clim Dyn 40:2123–2165

(EC-Earth) E-EC, (2019) EC-earth-consortium EC-Earth3 model output prepared for CMIP6 CMIP historical. Earth Syst Grid Fed. https://doi.org/10.22033/ESGF/CMIP6.4700

(EC-Earth) E-EC, (2019) EC-Earth-Consortium EC-Earth3-Veg model output prepared for CMIP6 ScenarioMIP. Earth Syst Grid Fed. https://doi.org/10.22033/ESGF/CMIP6.727

(EC-Earth) E-EC, (2021) EC-Earth-Consortium EC-Earth-3-CC model output prepared for CMIP6 CMIP historical. Earth Syst Grid Fed. https://doi.org/10.22033/ESGF/CMIP6.4702

Edomah N, Ndulue G, Lemaire X (2021) A review of stakeholders and interventions in nigeria's electricity sector. Heliyon 7(9):07956

El Mghouchi Y, Ajzoul T, El Bouardi A (2016) Prediction of daily solar radiation intensity by day of the year in twenty-four cities of morocco. Renew Sustain Energy Rev 53:823–831

Eyring V, Bony S, Meehl GA, Senior CA, Stevens B, Stouffer RJ, Taylor KE (2016) Overview of the coupled model intercomparison project phase 6 (cmip6) experimental design and organization. Geosci Model Dev 9(5):1937–1958

Galin VY (1998) Parametrization of radiative processes in the dnm atmospheric model. Izvestiya Akademii Nauk-Rossijskaya Akademiya Nauk. Fizika Atmos i Okeana 34

(GERICS) CSCG (2017) MPI-CSC CORDEX data for Africa (AFR-44) based on REMO2009 model simulations. World Data Center for Climate (WDCC) at DKRZ. http://cera-www.dkrz.de/WDCC/ui/Compact.jsp?acronym=CXAF44MCR1

He B, Bao Q, Wang X, Zhou L, Wu X, Liu Y, Wu G, Chen K, He S, Hu W et al (2019) Cas fgoals-f3-l model datasets for cmip6 historical atmospheric model intercomparison project simulation. Adv Atmos Sci 36:771–778

Heo K-Y, Ha K-J, Yun K-S, Lee S-S, Kim H-J, Wang B (2014) Methods for uncertainty assessment of climate models and model predictions over east asia. Int J Climatol 34(2):377–390

Hersbach H, Bell B, Berrisford P, Hirahara S, Horányi A, Muñoz-Sabater J, Nicolas J, Peubey C, Radu R, Schepers D et al (2020) The era5 global reanalysis. Q J R Meteorol Soc 146(730):1999–2049

Hogan RJ, Ahlgrimm M, Balsamo G, Beljaars A, Berrisford P, Bozzo A, Di Giuseppe F, Forbes RM, Haiden T, Lang S *et al* (2017) Radiation in Numerical Weather Prediction. Eur Centre Medium-Range Weather Forecast

Huang W (2019) THU CIESM model output prepared for CMIP6 ScenarioMIP. Earth Syst Grid Fed. https://doi.org/10.22033/ESGF/CMIP6.1357

Iacono MJ, Delamere JS, Mlawer EJ, Shephard MW, Clough SA, Collins WD (2008) Radiative forcing by long-lived greenhouse gases: calculations with the aer radiative transfer models. J Geophys Res Atmos. https://doi.org/10.1029/2008JD009944

Iwayemi A, Iwayemi A (1998) Energy Sect Dev Afr. African development bank

Ji D, Wang L, Feng J, Wu Q, Cheng H, Zhang Q, Yang J, Dong W, Dai Y, Gong D et al (2014) Description and basic evaluation of beijing normal university earth system model (bnu-esm) version 1. Geosci Model Dev 7(5):2039–2064

Jiang H, Lu N, Yao L, Qin J, Liu T (2023) Impact of climate changes on the stability of solar energy: evidence from observations and reanalysis. Renew Energy 208:726–736

(KNMI) RNMI (2017) KNMI CORDEX data for Africa (AFR-44) based on RACMO22T model simulations. World Data Center for Climate (WDCC) at DKRZ. http://cera-www.dkrz.de/WDCC/ui/Compact.jsp?acronym=CXAF44KNRT

Lee W-L, Liang H-C (2020) AS-RCEC TaiESM1.0 model output prepared for CMIP6 CMIP historical. Earth Syst Grid Fed. https://doi.org/10.22033/ESGF/CMIP6.9755

Lee W-L, Wang Y-C, Shiu C-J, Tsai I-C, Tu C-Y, Lan Y-Y, Chen J-P, Pan H-L, Hsu H-H et al (2020) Taiwan earth system model version 1: description and evaluation of mean state. Geosci Model Dev 13(9):3887–3904

Lin Y, Huang X, Liang Y, Qin Y, Xu S, Huang W, Xu F, Liu L, Wang Y, Peng Y et al (2020) Community integrated earth system model (ciesm): description and evaluation. J Adv Model Earth Syst 12(8):2019–002036

Liu Z, Yang X, Xie R, Lin X, Li T, Batchelor WD, Zhao J, Zhang Z, Sun S, Zhang F et al (2021) Prolongation of the grain filling period and change in radiation simultaneously increased maize yields in china. Agric For Meteorol 308:108573

Long MC, Lindsay K, Peacock S, Moore JK, Doney SC (2013) Twentieth-century oceanic carbon uptake and storage in cesm1 (bgc). J Clim 26(18):6775–6800

Lovato T, Peano D (2020) CMCC CMCC-CM2-SR5 model output prepared for CMIP6 ScenarioMIP. Earth Syst Grid Fed. https://doi.org/10.22033/ESGF/CMIP6.1365

Lovato T, Peano D, Butenschön M (2021) CMCC CMCC-ESM2 model output prepared for CMIP6 CMIP historical. Earth Syst Grid Fed. https://doi.org/10.22033/ESGF/CMIP6.13195

Lovato T, Peano D, Butenschön M, Materia S, Iovino D, Scoccimarro E, Fogli P, Cherchi A, Bellucci A, Gualdi S et al (2022) Cmip6 simulations with the cmcc earth system model (cmcc-esm2). J Adv Model Earth Syst 14(3):2021–002814

Lu Y, Wang L, Zhu C, Zou L, Zhang M, Feng L, Cao Q (2023) Predicting surface solar radiation using a hybrid radiative transfer-machine learning model. Renew Sustain Energy Rev 173:113105

Matthes K, Funke B, Andersson ME, Barnard L, Beer J, Charbonneau P, Clilverd MA, Dudok de Wit T, Haberreiter M, Hendry A, Jackman CH, Kretzschmar M, Kruschke T, Kunze M, Langematz U, Marsh DR, Maycock AC, Misios S, Rodger CJ, Scaife AA, Seppälä A, Shangguan M, Sinnhuber M, Tourpali K, Usoskin I, van de Kamp M, Verronen PT, Versick S (2017) Solar forcing for cmip6 (v3.2). Geosci Model Dev 10(6):2247–2302. https://doi.org/10.5194/gmd-10-2247-2017

Meng Q, Liu B, Yang H, Chen X (2020) Solar dimming decreased maize yield potential on the north china plain. Food and Energy Secur 9(4):235

Meteorological S, (SMHI) HI (2017) cordex AFR-44 SMHI RCA4. World Data Center for Clim http://cera-www.dkrz.de/WDCC/ui/Compact.jsp?acronym=CXAF44SMRCA4

Mlawer EJ, Taubman SJ, Brown PD, Iacono MJ, Clough SA (1997) Radiative transfer for inhomogeneous atmospheres: Rrtm, a validated correlated-k model for the longwave. J Geophys Res Atmos 102(D14):16663–16682

Neale R, Gettelman A, Park S, Chen C, Lauritzen P, Williamson D, Conley A, Kinnison D, Marsh D, Smith A et al (2010) Description of the ncar community atmosphere model (cam 5.0), ncar tech note tn-486. Nat Center Atmos Res. https://doi.org/10.5065/wgtk-4g06

Nešović AM (2022) Comparison of theoretical and isotropic models of incoming solar radiation for the tilted, fixed, flat-plate solar collector southoriented. Tehnika 77(5):553–558

Ogunjo ST, Olusegun CF, Fuwape IA (2022) Evaluation of monthly precipitation data from three gridded climate data products over nigeria. Remote Sens Earth Syst Sci 5:119

Ojo OS, Adeyemi B, Ogolo EO (2021) Geostatistical distribution of net radiation at different sky conditions over west africa. Earth Syst Environ 5(1):43–57

Panitz H-J, Schubert-Frisius M, Dosio A (2015) CORDEX simulations (evaluation, historical, rcp85, and rcp45) on a ca 50 km grid over Africa based on CCLM4-8-17 forced by MPI-ESM-LR, EC-EARTH, CNRM-CM5 and HadGEM2-ES. World Data Center for Clim. https://doi.org/10.1594/WDCC/CXAF44CLCL

Patchali TE, Ajide OO, Matthew OJ, Salau T, Oyewola OM (2020) Examination of potential impacts of future climate change on solar radiation in togo, west africa. SN Appl Sci 2:1–13

Pincus R, Barker HW, Morcrette J-J (2003) A fast, flexible, approximate technique for computing radiative transfer in inhomogeneous cloud fields. J Geophys Res Atmos. https://doi.org/10.1029/2002JD003322

Qiao F, Song Z, Bao Y, Song Y, Shu Q, Huang C, Zhao W (2013) Development and evaluation of an earth system model with surface gravity waves. J Geophys Res Oceans 118(9):4514–4524

Sabah F, Salmn M (2021) Modeling of global solar radiation in algeria based on geographical and all climatic parameters. Int J Comput Exp Sci Eng 7(3):119–122

Salaudeen A, Ismail A, Adeogun B, Ajibike M (2021) Validating gauge-based spatial surface atmospheric temperature datasets for upper Benue river Basin, Nigeria. Niger J Environ Sci Technol 5(1):173–190

Schmidt GA, Kelley M, Nazarenko L, Ruedy R, Russell GL, Aleinov I, Bauer M, Bauer SE, Bhat MK, Bleck R et al (2014) Configuration and assessment of the giss modele2 contributions to the cmip5 archive. J Adv Model Earth Syst 6(1):141–184

Seland Ø, Bentsen M, Oliviè DJL, Toniazzo T, Gjermundsen A, Graff LS, Debernard JB, Gupta AK, He Y-C, Kirkevåg A et al (2020) Overview of the norwegian earth system model (noresm2) and key climate response of cmip6 deck, historical, and scenario simulations. Geosci Model Dev 13:6165

Smith CJ, Forster PM (2021) Suppressed late-20th century warming in cmip6 models explained by forcing and feedbacks. Geophys Res Lett 48(19):2021–094948

Solomon S (2007) Climate Change 2007-the Physical Science Basis: Working Group I Contribution to the Fourth Assessment Report of the IPCC vol. 4. Cambridge university press

Song Z, Qiao F, Bao Y, Shu Q, Song Y, Yang X (2019) FIO-QLNM FIO-ESM2.0 model output prepared for CMIP6 CMIP historical. Earth Syst Grid Fed. https://doi.org/10.22033/ESGF/CMIP6.9199

Tahir Z.u.R., Azhar M, Mumtaz M, Asim M, Moeenuddin G, Sharif H, Hassan S (2020) Evaluation of the reanalysis surface solar radiation from ncep, ecmwf, nasa, and jma using surface observations for balochistan, pakistan. J Renew Sustain Energy 12(2):023703

Tang W, Qin J, Yang K, Zhu F, Zhou X (2021) Does era5 outperform satellite products in estimating atmospheric downward longwave radiation at the surface? Atmos Res 252:105453

Taylor KE (2001) Summarizing multiple aspects of model performance in a single diagram. J Geophys Res Atmos 106(D7):7183–7192
Taylor KE (2001) Summarizing multiple aspects of model performance in a single diagram. J Geophys Res Atmos 106(D7):7183–7192
Taylor KE, Stouffer RJ, Meehl GA (2012) An overview of cmip5 and the experiment design. Bull Am Meteor Soc 93(4):485–498
Trolliet M, Walawender JP, Bourlès B, Boilley A, Trentmann J, Blanc P, Lefèvre M, Wald L (2018) Downwelling surface solar irradiance in the tropical atlantic ocean: a comparison of re-analyses and satellite-derived data sets to pirata measurements. Ocean Sci 14(5):1021–1056
Urraca R, Huld T, Gracia-Amillo A, Martinez-de-Pison FJ, Kaspar F, Sanz-Garcia A (2018) Evaluation of global horizontal irradiance estimates from era5 and cosmo-rea6 reanalyses using ground and satellite-based data. Sol Energy 164:339–354
Voldoire A, Sanchez-Gomez E, Salas y Mélia D, Decharme B, Cassou C, Sénési S, Valcke S, Beau I, Alias A, Chevallier M et al (2013) The cnrm-cm5. 1 global climate model: description and basic evaluation. Clim Dyn 40:2091–2121
Volodin E, Dianskii N, Gusev A (2010) Simulating present-day climate with the inmcm4. 0 coupled model of the atmospheric and oceanic general circulations. Izv Atmos Ocean Phys 46:414–431
Volodin E, Mortikov E, Kostrykin S, Galin VY, Lykossov V, Gritsun A, Diansky N, Gusev A, Iakovlev N (2017) Simulation of the present-day climate with the climate model inmcm5. Clim Dyn 49:3715–3734
Volodin E, Mortikov E, Gritsun A, Lykossov V, Galin V, Diansky N, Gusev A, Kostrykin S, Iakovlev N, Shestakova A et al (2019) Cmip6. scenariomip. inm. inm-cm5-0. ssp585
von Storch J-S, Putrasahan D, Lohmann K, Gutjahr O, Jungclaus J, Bittner M, Haak H, Wieners K-H, Giorgetta M, Reick C, Esch M, Gayler V, de Vrese P, Raddatz T, Mauritsen T, Behrens J, Brovkin V, Claussen M, Crueger T, Fast I, Fiedler S, Hagemann S, Hohenegger C, Jahns T, Kloster S, Kinne S, Lasslop G, Kornblueh L, Marotzke J, Matei D, Meraner K, Mikolajewicz U, Modali K, Müller W, Nabel J, Notz D, Peters-von Gehlen K, Pincus R, Pohlmann H, Pongratz J, Rast S, Schmidt H, Schnur R, Schulzweida U, Six K, Stevens B, Voigt A, Roeckner E (2017) MPI-M MPIESM1.2-HR model output prepared for CMIP6 HighResMIP. Earth Syst Grid Fed. https://doi.org/10.22033/ESGF/CMIP6.762
Wang S-Y, Qiu J, Li F-F (2018) Hybrid decomposition-reconfiguration models for long-term solar radiation prediction only using historical radiation records. Energies 11(6):1376
Wang Z, Wang C, Yang S, Lei Y, Che H, Zhang X, Wang Q (2022) Evaluation of surface solar radiation trends over china since the 1960s in the cmip6 models and potential impact of aerosol emissions. Atmos Res 268:105991
Wu J, Han Z, Yan Y, Gao X (2022) Future projection of solar energy over china based on multi-regional climate model simulations. Earth Space Sci 9(5):2021–002207
Xin X, Zhang J, Zhang F, Wu T, Shi X, Li J, Chu M, Liu Q, Yan J, Ma Q, Wei M (2018) BCC BCC-CSM2MR model output prepared for CMIP6 CMIP. Earth Syst Grid Fed. https://doi.org/10.22033/ESGF/CMIP6.1725
Yang Q, Zhang F, Zhang H, Wang Z, Iwabuchi H, Li J (2020) Impact of $\delta$-four-stream radiative transfer scheme on global climate model simulation. J Quant Spectrosc Radiat Transfer 243:106800
Yu Y (2019) Cas fgoals-f3-l model output prepared for cmip6 scenariomip. Version 532:20191204
Yukimoto S, Adachi Y, Hosaka M, Sakami T, Yoshimura H, Hirabara M, Tanaka TY, Shindo E, Tsujino H, Deushi M, Mizuta R, Yabu S, Obata A, Nakano H, Koshiro T, Ose T, Kitoh A (2012) A new global climate model of the meteorological research institute: Mri-cgcm3;model description and basic performance. J Meteorol Soc Jpn Ser II 90A:23–64. https://doi.org/10.2151/jmsj.2012-A02
Yukimoto S, Koshiro T, Kawai H, Oshima N, Yoshida K, Urakawa S, Tsujino H, Deushi M, Tanaka T, Hosaka M, Yoshimura H, Shindo E, Mizuta R, Ishii M, Obata A, Adachi Y (2019) MRI MRI-ESM2.0 model output prepared for CMIP6 CMIP. Earth Syst Grid Fed. https://doi.org/10.22033/ESGF/CMIP6.621
Yukimoto S, Kawai H, Koshiro T, Oshima N, Yoshida K, Urakawa S, Tsujino H, Deushi M, Tanaka T, Hosaka M et al (2019) The meteorological research institute earth system model version 2.0, mri-esm2. 0: description and basic evaluation of the physical component. J Meteorol Soc Jpn Ser II 97(5):931–965
Zanchettin D, Rubino A, Matei D, Bothe O, Jungclaus J (2013) Multidecadal-to-centennial sst variability in the mpi-esm simulation ensemble for the last millennium. Clim Dyn 40:1301–1318
Zhang F, Li J (2013) Doubling-adding method for delta-four-stream spherical harmonic expansion approximation in radiative transfer parameterization. J Atmos Sci 70(10):3084–3101
Zhang H, Zhang M, Jin J, Fei K, Ji D, Wu C, Zhu J, He J, Chai Z, Xie J et al (2020) Description and climate simulation performance of cas-esm version 2. J Adv Model Earth Syst 12(12):2020–002210
Zhou Y, Liu Y, Wang D, De G, Li Y, Liu X, Wang Y (2021) A novel combined multi-task learning and gaussian process regression model for the prediction of multi-timescale and multi-component of solar radiation. J Clean Prod 284:124710